

Cite this: *RSC Adv.*, 2018, **8**, 10593

Received 19th December 2017  
 Accepted 12th February 2018

DOI: 10.1039/c7ra13443f

rsc.li/rsc-advances

## Interface engineering of graphene–silicon Schottky junction solar cells with an $\text{Al}_2\text{O}_3$ interfacial layer grown by atomic layer deposition

Aaesha Alnuaimi,<sup>a</sup> <sup>\*ab</sup> Ibraheem Almansouri,<sup>b</sup> Irfan Saadat<sup>b</sup> and Ammar Nayfeh<sup>b</sup>

The recent progress in graphene (Gr)/silicon (Si) Schottky barrier solar cells (SBSC) has shown the potential to produce low cost and high efficiency solar cells. Among the different approaches to improve the performance of Gr/Si SBSC is engineering the interface with an interfacial layer to reduce the high recombination at the graphene (Gr)/silicon (Si) interface and facilitate the transport of photo-generated carriers. Herein, we demonstrate improved performance of Gr/Si SBSC by engineering the interface with an aluminum oxide ( $\text{Al}_2\text{O}_3$ ) layer grown by atomic layer deposition (ALD). With the introduction of an  $\text{Al}_2\text{O}_3$  interfacial layer, the Schottky barrier height is increased from 0.843 V to 0.912 V which contributed to an increase in the open circuit voltage from 0.45 V to 0.48 V. The power conversion efficiency improved from 7.2% to 8.7% with the  $\text{Al}_2\text{O}_3$  interfacial layer. The stability of the Gr/ $\text{Al}_2\text{O}_3$ /Si devices was further investigated and the results have shown a stable performance after four weeks of operation. The findings of this work underpin the potential of using an  $\text{Al}_2\text{O}_3$  interfacial layer to enhance the performance and stability of Gr/Si SBSC.

## 1. Introduction

The high cost and inadequate efficiency of existing solar cell technologies have caused current efforts to focus on investigating new materials to achieve low cost and high efficiency solar cells. Graphene is one of the most promising materials that has attracted a tremendous amount of attention in the photovoltaics field due to its unique properties, being a two-dimensional material with near-zero bandgap and highly transparent film with excellent electrical conductivity. Graphene has been utilized in various PV technologies as a transparent electrode, electron and hole transport layer in organic solar cells and catalyst in dye sensitized solar cells (DSSCs).<sup>1–8</sup> The recent development of Gr/silicon (Si) Schottky barrier solar cells (SBSC) have shown a great potential to produce low cost and high efficiency solar cells with the highest reported efficiency being 15.6%.<sup>9,10</sup> Despite the recent efforts in enhancing the electrical and optical performance of Gr/Si SBSC,<sup>9–23</sup> further performance optimization is required. The performance of Gr/Si SBSC is highly affected by the high recombination at Gr/Si interface and the continues but non-uniform growth of native oxide that prevents the tunnelling of the photo-generated charge carriers and leading to performance degradation and

instability issues. Such behaviour has been observed for metal/Si interface and among the different approaches that have been adopted to reduce the recombination and enhance the interface properties is engineering the interface with interfacial layers.<sup>24–27</sup> Previous studies on Gr/Si SBSC have shown an improved performance of Gr/Si SBSC by introducing solution based interfacial layers to improve Gr/Si interface.<sup>15,18,19,21,22</sup> However, some of the undesirable properties of solution processed materials are the difficulty in obtaining uniform coating and controlling the thickness precisely which are important properties to obtain good passivation at the interface that doesn't affect the tunnelling of the charge carriers. The ALD technique is an excellent choice for the deposition of high quality thin film owing to the ability of obtaining conformal coating and controlling the thickness and composition at the atomic level. Herein, we analyzed the effect of  $\text{Al}_2\text{O}_3$  grown by ALD as interfacial layer for Gr/Si SBSC.

## 2. Experimental methods

### 2.1 Graphene synthesis

A high quality monolayer graphene with sheet resistance of  $\sim 650 \Omega \text{ sq}^{-1}$  was grown on copper foil using chemical vapour deposition using Aixtron cold wall CVD reactor. The growth was done using a mixture of methane  $\text{CH}_4$  (15 sccm) and hydrogen  $\text{H}_2$  (60 sccm) at 1060 °C and pressure of 15 mbar. Further details about the synthesis can be found in ref. 28. The formation of high quality monolayer graphene was examined using Raman analysis. Fig. 1 shows the Raman spectrum of as-synthesized

<sup>a</sup>Research and Development Centre, Dubai Electricity and Water Authority (DEWA), Dubai, United Arab Emirates

<sup>b</sup>Department of Electrical and Computer Engineering (ECE), Masdar Institute, Khalifa University of Science and Technology, P. O. Box 54224, Abu Dhabi, United Arab Emirates. E-mail: aar.alnuaimi@gmail.com

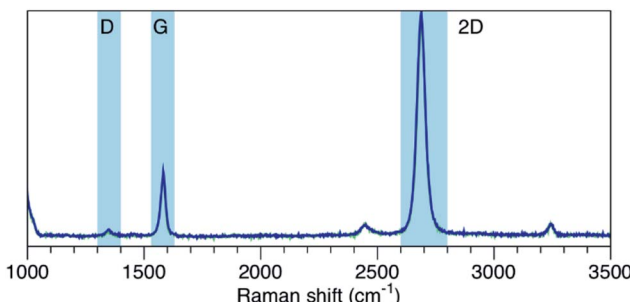


Fig. 1 Raman spectrum of synthesized graphene.<sup>28</sup>

graphene. The ratio of 2D-band peak ( $2682\text{ cm}^{-1}$ ) to G-band peak ( $1580\text{ cm}^{-1}$ )  $I_{2D}/I_G$  is greater than two which confirms the formation of a monolayer graphene. The weak D-band peak ( $1350\text{ cm}^{-1}$ ) suggests the high quality of the grown graphene.

## 2.2 Gr/Si solar cells fabrication

The fabrication steps of Gr/Si SBSC are illustrated in Fig. 2. Twelve solar cells with active area of  $2 \times 2\text{ mm}$  were fabricated using lightly doped n-type Si substrate with resistivity of  $3\text{--}4\text{ }\Omega\text{ cm}$ . A  $300\text{ nm}$  silicon oxide was deposited on top of the silicon substrate to define the active area. Using lithography, a window was patterned and the silicon oxide was etched using buffered oxide etch (BOE) to expose the underlying silicon which defines the size of the solar cell. After the etching step, the samples were transferred to the Oxford instruments FlexAL ALD reactor for  $\text{Al}_2\text{O}_3$  deposition.

A thin layer of  $\text{Al}_2\text{O}_3$  oxide was deposited using thermal ALD at low temperature of  $300\text{ }^\circ\text{C}$  and pressure of  $200\text{ mTorr}$ . Trimethylaluminum (TMA,  $\text{Al}(\text{CH}_3)_3$ ) was used as the gas precursor for Al while  $\text{H}_2\text{O}$  is used the oxygen precursor. The estimated deposition rate is  $1\text{ \AA}$  per cycle and the estimated thickness is  $\sim 20\text{ \AA}$ . The ALD step was followed by graphene transfer. Two layers of graphene were transferred using the standard PMMA (poly(methyl methacrylate)) transfer process. The samples were exposed to the vapour of nitric acid for  $1\text{ min}$  to dope the

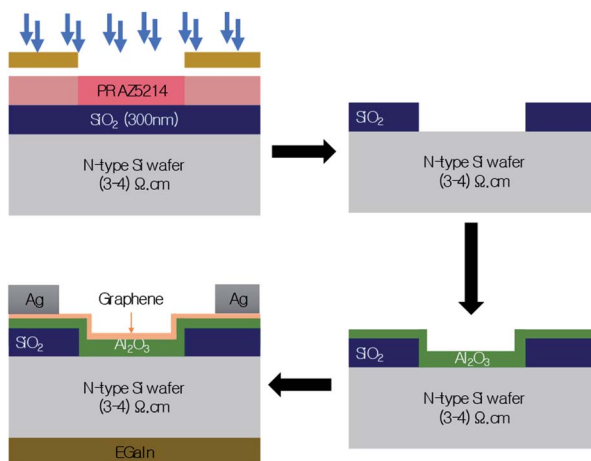


Fig. 2 Schematic diagram of Gr/Al<sub>2</sub>O<sub>3</sub>/Si solar cell fabrication steps.

graphene. Gallium-indium eutectic (Ga-In 99.99%) was used as the back silicon contact while silver (Ag) paste was applied around the active area to contact the graphene.

## 2.3 Gr/Si solar cells characterization

Sol3A 94123A solar simulator was used to measure the current-voltage characteristics of the fabricated cells under 1 sun illumination. A black tape was used to cover the solar cell except at the active area to avoid any current collected from surrounding area. The light intensity of the simulator was calibrated using silicon reference cell and irradiance monitor. Agilent Probe analyser was used for the dark current measurements.

## 3. Results and discussion

Fig. 3 illustrates the current density–voltage ( $J$ – $V$ ) curves under AM1.5 illumination conditions of Gr/Si solar cells with and without  $\text{Al}_2\text{O}_3$  interfacial layer. In the absence of  $\text{Al}_2\text{O}_3$  interfacial layer, the short circuit current density ( $J_{sc}$ ), open circuit voltage ( $V_{oc}$ ) and fill factor (FF) of Gr/Si solar cell are  $27.7\text{ mA cm}^{-2}$ ,  $0.45\text{ V}$ ,  $58.3\%$ . With the introduction of  $\text{Al}_2\text{O}_3$  interfacial layer, the performance of the cell improved significantly. The  $J_{sc}$ ,  $V_{oc}$ , and FF increased to  $28.8\text{ mA cm}^{-2}$ ,  $0.48\text{ V}$ ,  $63.75\%$  leading to an enhancement in the power conversion efficiency from  $7.2\%$  to  $8.7\%$ . Table 1 shows the average value of performance parameters of devices fabricated with and without  $\text{Al}_2\text{O}_3$  passivation layer. Fig. 4 shows the histogram of keys performance parameters ( $V_{oc}$ ,  $J_{sc}$ , FF and PCE) for Gr/Si solar cells with  $\text{Al}_2\text{O}_3$  interfacial layer.

One of the main factors that contributed to the improvement in the solar cell performance with the addition of  $\text{Al}_2\text{O}_3$  interfacial layer is the increase in the Schottky barrier height (SBH). The SBH was extracted from the slope of the dark  $\ln(J)$ – $V$  curve at the forward bias linear region as illustrated in Fig. 3a. For Gr/Si solar cells without  $\text{Al}_2\text{O}_3$ , the estimated SBH is  $0.843\text{ V}$  and it increased to  $0.921\text{ V}$  with  $\text{Al}_2\text{O}_3$  interfacial layer. The increase in the barrier height at the interface blocks the transport of the photo-generated electrons in silicon hence reducing the leakage current. As illustrated in Fig. 5a, the reverse saturation current

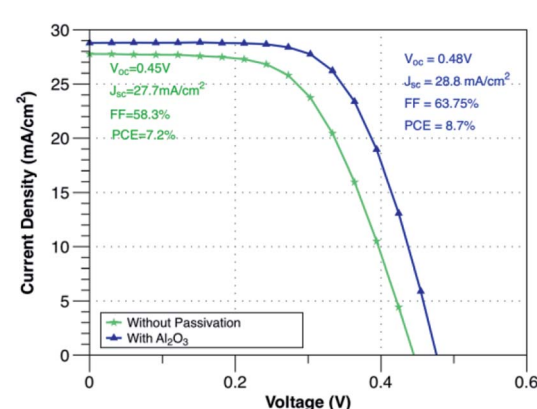
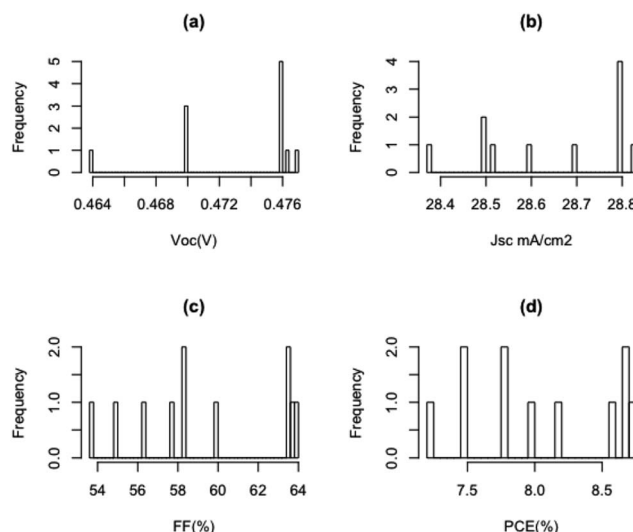


Fig. 3  $J$ – $V$  characteristics of Gr/Si solar cells with and without  $\text{Al}_2\text{O}_3$  interfacial layer.



**Table 1** Summary of performance parameters of devices fabricated with and without  $\text{Al}_2\text{O}_3$  passivation layer

Solar cell	$V_{\text{oc}}$ (V)	$J_{\text{sc}}$ mA cm $^{-2}$	FF (%)	PCE (%)
Without passivation	0.43	27.7	53.9	6.4
With $\text{Al}_2\text{O}_3$	0.47	28.6	59.2	8.0



**Fig. 4** Histogram of (a) open circuit voltage (b) short circuit current (c) fill factor (d) power conversion efficiency for Gr/Si solar cells with  $\text{Al}_2\text{O}_3$  interfacial layer.

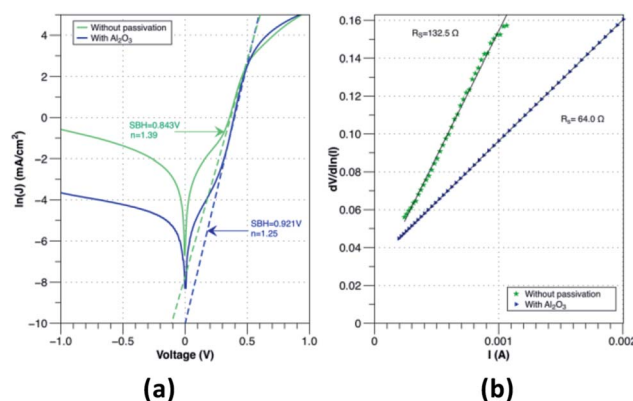


**Fig. 5** (a) Dark J-V characteristics of Gr/Si solar cells with and without  $\text{Al}_2\text{O}_3$  interfacial layer. Inset shows the corresponding  $\ln J$ -V curves. (b) Plots of  $dV/d\ln(I)$  versus  $I$  for Gr/Si solar cells with and without  $\text{Al}_2\text{O}_3$  interfacial layer.

is reduced from  $4.50 \times 10^{-4}$  mA cm $^{-2}$  to  $4.48 \times 10^{-5}$  mA cm $^{-2}$  while the ideality factor ( $n$ ) is reduced from 1.39 to 1.25 confirming the significant reduction in the recombination of carriers. Furthermore, the increase in the SBH also indicates the creation of larger built-in potential ( $V_{\text{bi}}$ ) across the depletion region that is beneficial for enhancing the transfer of the carriers at the interface. The  $V_{\text{bi}}$  of the solar cell has been extracted from the crossover between the IV characteristics under illumination and dark condition<sup>29</sup> and it was found that

$V_{\text{bi}}$  increased from 0.54 V to 0.58 V with  $\text{Al}_2\text{O}_3$ . The strong dependence of  $V_{\text{oc}}$  on the SBH as described in eqn (1) as well as the reduction in the dark current and ideality factor clearly explains the increase in the  $V_{\text{oc}}$  with the introduction of  $\text{Al}_2\text{O}_3$  interfacial layer.

$$V_{\text{oc}} = \frac{n k T}{q} \ln \left( \frac{J_{\text{ph}}}{A T^2} \right) + \frac{n}{q} (\text{SBH}) \quad (1)$$

In addition, the series resistance  $R_s$  was extracted by plotting the curve of  $dV/d\ln(I)$  as a function of  $I$  and estimating the  $R_s$  value from the slope of the linear fitting to the curves to the curves (Fig. 5b). The series resistance dropped from  $132.5 \Omega$  to  $64.0 \Omega$  which results in improving the fill factor with  $\text{Al}_2\text{O}_3$  interlayer.

The benefits of  $\text{Al}_2\text{O}_3$  interfacial layers is not only limited to creating higher Schottky barrier but it also reduces the recombination at the interface. In SBSC the tunnelling of holes should dominates over the recombination to achieve effective charge carrier transport. According to Song *et al.*<sup>9</sup> the existence of ultra-thin layer of native oxide passivates the interface between the graphene and silicon and allows the tunnelling of holes. However, since the native oxide thickness tends grow continuously, the performance of Gr/Si solar cell degrades with time. As shown in Fig. 6a, due to the increase in the native oxide thickness, the tunnelling of holes is reduced causing accumulation at the interface which consequently results in higher recombination of charge carriers. Therefore, the use of  $\text{SiO}_2$  interfacial layer has major issues that affect the performance stability of the Gr/Si SBSC. In contrast,  $\text{Al}_2\text{O}_3$  has been proven as a good passivation layer for Si substrate.<sup>30-33</sup> As shown in Fig. 6b, passivating the surface with  $\text{Al}_2\text{O}_3$  immediately after the native oxide etch prevents the formation of thick native oxide at the

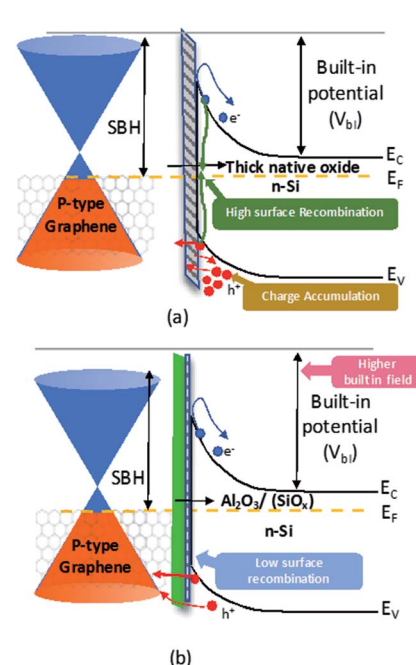


**Fig. 6** Energy band diagrams of Gr/Si SBSC (a) with thick interfacial layer (b) with  $\text{Al}_2\text{O}_3$ /native oxide interfacial layers.

interface. In addition, it creates a uniform and conformal  $\text{Al}_2\text{O}_3$  layer that passivates the Si surface effectively. The formation of uniform ultra-thin  $\text{Al}_2\text{O}_3$  layer contributed to reducing the surface recombination, improving the carrier lifetime for Si substrate and reducing the series resistance. According to Hoex *et al.*<sup>30</sup> passivating the Si surface with  $\text{Al}_2\text{O}_3$  reduces the density of traps significantly causing a major reduction in the surface recombination. Therefore, the enhancement of the solar cell performance with  $\text{Al}_2\text{O}_3$  interfacial layer is mainly attributed to passivating the silicon surface that reduces the surface recombination and the creation of higher SBH that facilitates the transport of charge carrier effectivity.

The stability of the cell was examined over four weeks as shown in Fig. 7. There was an observed degradation in the performance of the cell after one week. The drop in the efficiency and  $V_{\text{oc}}$  after one week is mainly attributed to the degradation effect of nitric acid dopant as observed by Cui *et al.*<sup>13</sup> The nitrite anions in nitric acid acts as a p-type dopant to the graphene (*i.e.* increasing the work function of the graphene) and reduces its sheet resistance. Upon the degradation of the dopant, the graphene work function decreases and the sheet resistance increases which results in a large drop in the efficiency and  $V_{\text{oc}}$ .

After four weeks, there was no observed major degradation in the cell performance. This highlights the benefit of using  $\text{Al}_2\text{O}_3$  as a passivation layer and blocking layer since it prevents further growth of native oxide and helps the cell to maintain its performance. The slight reduction in the PCE from 6.9% in week 1 to 6.6% in week 4 is mainly attributed to the reduction in FF from 54.12% to 52.10%. The contact series resistance increased due to the use of silver paste as the top contact. The silver paste degrades more compared to thermally vacuum evaporated front contacts which mainly impact the series resistance and causes a reduction in the fill factor of the cell.<sup>34</sup>

Possible routes to further improve the efficiency of Gr/Si SBSC with  $\text{Al}_2\text{O}_3$  layer is to investigate the effect of  $\text{Al}_2\text{O}_3$  oxide and find the optimal thickness that maximize the cell efficiency. According to Song *et al.*<sup>9</sup> increasing the interfacial layer thickness can further reduce the leakage current and contributes to increasing the  $V_{\text{oc}}$ . However, with further increase in the interfacial layer beyond the optimal thickness, the tunnelling probability is reduced by the factor  $\exp(-\sqrt{\chi}d)$  where  $\chi$  is the average

potential barrier of the oxide for hole tunnelling into the graphene and  $d$  is the interfacial layer thickness. Due to the reduction in the tunnelling probability, the charge carriers accumulate at the interface and results in increasing the recombination rate.

## 4. Conclusions

In conclusion, the use of  $\text{Al}_2\text{O}_3$  interfacial layer to engineer the interface between the graphene and silicon is demonstrated. The existence of  $\text{Al}_2\text{O}_3$  interfacial layer mainly contributed to increasing the open circuit voltage and fill factor.  $\text{Al}_2\text{O}_3$  interfacial layer resulted in creating higher Schottky barrier height that is beneficial to increase the built-in potential and reduce recombination of charge carriers and leakage current. Solar cells with  $\text{Al}_2\text{O}_3$  showed an improvement in the power conversion efficiency from 7.2% to 8.7% and good stability over four weeks. The results highlight the potential of using  $\text{Al}_2\text{O}_3$  as interfacial layer for Gr/Si SBSC.

## Conflicts of interest

There are no conflicts to declare.

## Acknowledgements

The authors would like to acknowledge the valuable advice and constructive comments of Prof. Jing Kong and Yi-Song (from Massachusetts Institute of Technology) in graphene transfer as well as the fabrication of Gr/Si SBSC. This work is fully supported by Masdar Institute (part of Khalifa University of Science and Technology).

## References

- W. Hong, Y. Xu, G. Lu, C. Li and G. Shi, Transparent graphene/PEDOT-PSS composite films as counter electrodes of dye-sensitized solar cells, *Electrochim. Commun.*, 2008, **10**(10), 1555–1558.
- Z. Liu, J. Li, Z.-H. Sun, G. Tai, S.-P. Lau and F. Yan, The application of highly doped single-layer graphene as the top electrodes of semitransparent organic solar cells, *ACS Nano*, 2011, **6**(1), 810–818.
- H. Wang and Y. H. Hu, Graphene as a counter electrode material for dye-sensitized solar cells, *Energy Environ. Sci.*, 2012, **5**(8), 8182–8188.
- Y. Wang, S. W. Tong, X. F. Xu, B. Özyilmaz and K. P. Loh, Interface engineering of layer-by-layer stacked graphene anodes for high-performance organic solar cells, *Adv. Mater.*, 2011, **23**(13), 1514–1518.
- D. Zhang, X. Li, H. Li, S. Chen, Z. Sun, X. Yin, *et al.* Graphene-based counter electrode for dye-sensitized solar cells, *Carbon*, 2011, **49**(15), 5382–5388.
- Y. Zhou, X. Xu, F. Hu, X. Zheng, W. Li, P. Zhao, *et al.* Graphene as broadband terahertz antireflection coating, *Appl. Phys. Lett.*, 2014, **104**(5), 051106.

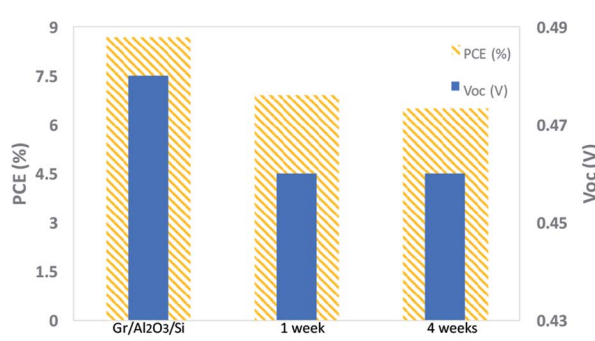


Fig. 7 Variation of PCE and  $V_{\text{oc}}$  of Gr/Si with  $\text{Al}_2\text{O}_3$  interfacial layer over time.



7 W. Yang, X. Xu, L. Hou, X. Ma, F. Yang, Y. Wang, *et al.* Insight into the topological defects and dopants in metal-free holey graphene for triiodide reduction in dye-sensitized solar cells, *J. Mater. Chem. A*, 2017, **5**(12), 5952–5960.

8 W. Yang, X. Xu, Y. Gao, Z. Li, C. Li, W. Wang, *et al.* High-surface-area nanomesh graphene with enriched edge sites as efficient metal-free cathodes for dye-sensitized solar cells, *Nanoscale*, 2016, **8**(26), 13059–13066.

9 Y. Song, X. Li, C. Mackin, X. Zhang, W. Fang, P. Ts, *et al.* Role of interfacial oxide in high-efficiency graphene–silicon Schottky barrier solar cells, *Nano Lett.*, 2015, **15**(3), 2104–2110.

10 X. Li, H. Zhu, K. Wang, A. Cao, J. Wei, C. Li, *et al.* Graphene-on-silicon Schottky junction solar cells, *Adv. Mater.*, 2010, **22**(25), 2743–2748.

11 X. Li, L. Fan, Z. Li, K. Wang, M. Zhong, J. Wei, *et al.* Boron Doping of Graphene for Graphene–Silicon p–n Junction Solar Cells, *Adv. Energy Mater.*, 2012, **2**(4), 425–429.

12 T. Feng, D. Xie, Y. Lin, H. Zhao, Y. Chen, H. Tian, *et al.* Efficiency enhancement of graphene/silicon-pillar-array solar cells by  $\text{HNO}_3$  and PEDOT-PSS, *Nanoscale*, 2012, **4**(6), 2130–2133.

13 T. Cui, R. Lv, Z.-H. Huang, S. Chen, Z. Zhang, X. Gan, *et al.* Enhanced efficiency of graphene/silicon heterojunction solar cells by molecular doping, *J. Mater. Chem. A*, 2013, **1**(18), 5736–5740.

14 Y. Tsuboi, F. Wang, D. Kozawa, K. Funahashi, S. Mouri, Y. Miyauchi, *et al.* Enhanced photovoltaic performances of graphene/Si solar cells by insertion of a  $\text{MoS}_2$  thin film, *Nanoscale*, 2015, **7**(34), 14476–14482.

15 K. Jiao, X. Wang, Y. Wang and Y. Chen, Graphene oxide as an effective interfacial layer for enhanced graphene/silicon solar cell performance, *J. Mater. Chem. C*, 2014, **2**(37), 7715–7721.

16 G. Fan, H. Zhu, K. Wang, J. Wei, X. Li, Q. Shu, *et al.* Graphene/silicon nanowire Schottky junction for enhanced light harvesting, *ACS Appl. Mater. Interfaces*, 2011, **3**(3), 721–725.

17 X. Miao, S. Tongay, M. K. Petterson, K. Berke, A. G. Rinzler, B. R. Appleton, *et al.* High efficiency graphene solar cells by chemical doping, *Nano Lett.*, 2012, **12**(6), 2745–2750.

18 S. Lin, X. Li, P. Wang, Z. Xu, S. Zhang, H. Zhong, *et al.* Interface designed  $\text{MoS}_2$ /GaAs heterostructure solar cell with sandwich stacked hexagonal boron nitride, *Sci. Rep.*, 2015, **5**, 15103.

19 L. Yang, X. Yu, M. Xu, H. Chen and D. Yang, Interface engineering for efficient and stable chemical-doping-free graphene-on-silicon solar cells by introducing a graphene oxide interlayer, *J. Mater. Chem. A*, 2014, **2**(40), 16877–16883.

20 X. Li, D. Xie, H. Park, M. Zhu, T. H. Zeng, K. Wang, *et al.* Ion doping of graphene for high-efficiency heterojunction solar cells, *Nanoscale*, 2013, **5**(5), 1945–1948.

21 K. Jiao, C. Duan, X. Wu, J. Chen, Y. Wang and Y. Chen, The role of  $\text{MoS}_2$  as an interfacial layer in graphene/silicon solar cells, *Phys. Chem. Chem. Phys.*, 2015, **17**(12), 8182–8186.

22 C. Xie, X. Zhang, Y. Wu, X. Zhang, X. Zhang, Y. Wang, *et al.* Surface passivation and band engineering: a way toward high efficiency graphene–planar Si solar cells, *J. Mater. Chem. A*, 2013, **1**(30), 8567–8574.

23 Y. Li, W. Yang, Z. Tu, Z. Liu, F. Yang, L. Zhang, *et al.* Schottky junction solar cells based on graphene with different numbers of layers, *Appl. Phys. Lett.*, 2014, **104**(4), 043903.

24 D. Lillington and W. Townsend, Effects of interfacial oxide layers on the performance of silicon Schottky-barrier solar cells, *Appl. Phys. Lett.*, 1976, **28**(2), 97–98.

25 Photocurrent suppression and interface state recombination in MIS-Schottky barriers, 1977 International Electron Devices Meeting, ed. Ng K. and Card H., 1977, pp. 57–61.

26 P. Viktorovitch and G. Kamarinos, Improvement of the photovoltaic efficiency of a metal-insulator-semiconductor structure: influence of interface states, *J. Appl. Phys.*, 1977, **48**(7), 3060–3064.

27 Determination of optimum parameters and characterization of MIS solar cells, 1977 International Electron Devices Meeting, ed. Viktorovitch P., Pananakakis G., Kamarinos G. and Basset R., 1977, pp. 62–62.

28 A. Alnuaimi, I. Almansouri, I. Saadat and A. Nayfeh, Toward fast growth of large area high quality graphene using a cold-wall CVD reactor, *RSC Adv.*, 2017, **7**(82), 51951–51957.

29 J. E. Moore, S. Dongaonkar, R. V. K. Chavali, M. A. Alam and M. S. Lundstrom, Correlation of built-in potential and  $I$ – $V$  crossover in thin-film solar cells, *IEEE Journal of Photovoltaics*, 2014, **4**(4), 1138–1148.

30 B. Hoex, S. Heil, E. Langereis, M. Van de Sanden and W. Kessels, Ultralow surface recombination of c-Si substrates passivated by plasma-assisted atomic layer deposited  $\text{Al}_2\text{O}_3$ , *Appl. Phys. Lett.*, 2006, **89**(4), 042112.

31 J. Schmidt, A. Merkle, R. Brendel, B. Hoex, M. Van De Sanden and W. Kessels, Surface passivation of high-efficiency silicon solar cells by atomic-layer-deposited  $\text{Al}_2\text{O}_3$ , *Progress in photovoltaics: research and applications*, 2008, **16**(6), pp. 461–466.

32 J. Deckers, E. Cornagliotti, M. Debucquoy, I. Gordon, R. Mertens and J. Poortmans, Aluminum oxide-aluminum stacks for contact passivation in silicon solar cells, *Energy Procedia*, 2014, **55**, 656–664.

33 J. Benick, B. Hoex, M. Van de Sanden, W. Kessels, O. Schultz and S. W. Glunz, High efficiency n-type Si solar cells on  $\text{Al}_2\text{O}_3$ -passivated boron emitters, *Appl. Phys. Lett.*, 2008, **92**(25), 253504.

34 A. R. Jha, *Solar cell technology and applications*, CRC press, 2009.

